Photoelectron Angular Distributions for Near-Threshold Two-Photon Ionization of Cesium and Rubidium Atoms

Adila Dodhy
Physics Department, Auburn University, Auburn, Alabama 36849, and Oak Ridge National Laboratory, Oak Ridge, Tennessee 37831

and

R. N. Compton and J. A. D. Stockdale
Chemical Physics Section, Health and Safety Research Division, Oak Ridge National Laboratory, Oak Ridge, Tennessee 37831
(Received 1 October 1984)

Photoelectron angular distributions have been measured for nonresonant two-photon ionization of cesium and rubidium atoms just above the ionization threshold. The photoelectron energies ranged from 25 to 100 meV. The results are compared with theoretical estimates based on nonrelativistic atomic wave functions. Initial results are also presented for above-threshold ionization in cesium.

PACS numbers: 32.80.Fb, 32.80.Rm

Multiphoton ionization (MPI) of atoms promises new insights into various problems of atomic structure and dynamics.[1-3] Perhaps the most powerful approach is the measurement of differential cross sections,[4-10] where the angular distributions of the photoejected electrons provide data not only on the magnitudes of the transition amplitudes but also on their relative phases. In addition to providing information about the scattering phase, thus complementing single-photon studies,[11] such measurements also test our theoretical understanding of high-order bound-free transitions involving sums over virtual intermediate states.[12]

Studies of photoelectron angular distributions for alkali-metal atoms have been limited to cases of resonantly enhanced MPI[4-6,8,10] or higher-order nonresonant processes.[7,12,13] In this paper, we report photoelectron angular distributions for nonresonant two-photon ionization of cesium and rubidium atoms where the photoejected electron has an energy in the range ~ 25–100 meV. Figure 1 shows the ionization scheme for both alkali metals. The first photon lies between the $6p$ and $7p$ states for cesium and between the $5p$ and $6p$ states for rubidium.

Our measurements are novel in two respects. First, we have studied photoelectron angular distributions in a region very close to the ionization threshold. This is difficult experimentally because of the very low energy of the photoelectrons under consideration. Second, we report photoelectron angular distributions for above-threshold ionization of cesium and compare them with theoretical predictions. Such processes have been observed by others in xenon[14-18] and cesium[13] but only in higher order (order 5 in cesium and ≥ 6 in xenon).

Details of the experimental apparatus have been described recently[10] in conjunction with resonantly enhanced MPI. Briefly, the output from a Nd:YAlG (yttrium aluminum garnet) pumped dye laser (Quanta Ray, DCR-II, PDL-I) was crossed orthogonally by a thermal alkali-metal beam. The dye-laser pulse duration was 5 ns and the bandwidth was 0.02 nm. The laser was focused to a power density of 10^8 W/cm^2 by a 35-mm lens. The power density was an order of magnitude greater when electrons from above-threshold ionization were studied. The plane of polarization of the laser was rotated by a double-Fresnel rhomb. Photoelectrons emerging perpendicular to the propagation vector of the laser beam and within $\pm 2°$ were energy analyzed by a 160° spherical-sector electrostatic energy analyzer. They were then detected by

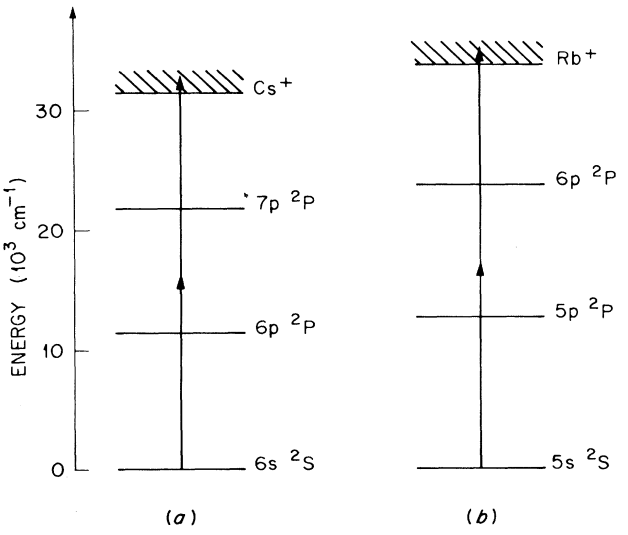

FIG. 1. Energy-level diagram showing the excitation scheme leading to ionization for nonresonant two-photon ionization of (a) cesium atoms and (b) rubidium atoms.

a dual-channelplate charged-particle detector, and the amplified signal was fed into a gated boxcar integrator (Princeton Applied Research, Model 162). Photoelectron angular distributions were obtained from a record of the relative photoelectron intensity as a function of the angle, θ, between the polarization of the laser and the fixed direction of detection of the photoelectrons. The laser–alkali-metal-atom interaction volume was carefully shielded from external electric and magnetic fields in order to detect the ultraslow photoelectrons. All critical surfaces were also coated with colloidal graphite in order to reduce surface potentials and electron reflection.

Cross sections for photoelectron angular distributions for two-photon ionization may be derived by use of time-dependent perturbation theory.[19,20] The resulting differential cross section, $\sigma(\theta)^{(2)}$, is given by

$$\sigma(\theta)^{(2)} = C^{(2)}(1+\beta_2^{(2)}\cos^2\theta+\beta_4^{(2)}\cos^4\theta), \quad (1)$$

where $C^{(2)}$ is a normalization constant. The coefficients $\beta_l^{(2)}$ are ratios of linear combinations of second-order radial matrix elements, $r_l^{(2)}$, and cosine functions of the difference in phase shifts between the allowed $l=0$ and $l=2$ continuum waves. The radial matrix elements are given by

$$r_l^{(2)} = \sum_{np} \frac{\langle kl|r|np\rangle\langle np|r|ns\rangle}{(E_{\text{g.s.}}-E_{np}+h\omega)}, \quad (2)$$

where $E_{\text{g.s.}}$ and E_{np} are the single-particle energies, ω is the frequency of the radiation field, k is the wave number of the photoelectron, and $\langle nl|r|nl'\rangle$ are radial dipole matrix elements. The radial wave functions for the ground states were generated in the nonrelativistic Hartree-Fock approximation. The sum over the virtual intermediate states, $|np\rangle$, found in Eq. (2) can be determined by any appropriate method. For the purposes of comparison with the experimental data, we will use the results of two independent calculations: (1) an analytic-expansion method based on a Sturmian basis set,[21–23] and (2) an inhomogeneous-differential-equation method[24–26] based on a Hartree-Fock potential.

The experimental and theoretical photoelectron angular distributions are shown in Fig. 2. The two-photon ionization threshold corresponds to a laser excitation wavelength of 636.8 nm for cesium and 593.6 nm for rubidium. The solid line through the experimental data points is the theoretical calculation using the Sturmian-basis-set method,[21] while the dashed curve is from the Hartree-Fock procedure.[24] The experimental and theoretical intensities are normalized to each other at $\theta=0°$. Good qualitative agreement is seen between the experimental measurements and theoretical calculations for both atoms. The experimental and theoretical values for the β coefficients are shown in Table I. The experimental values were

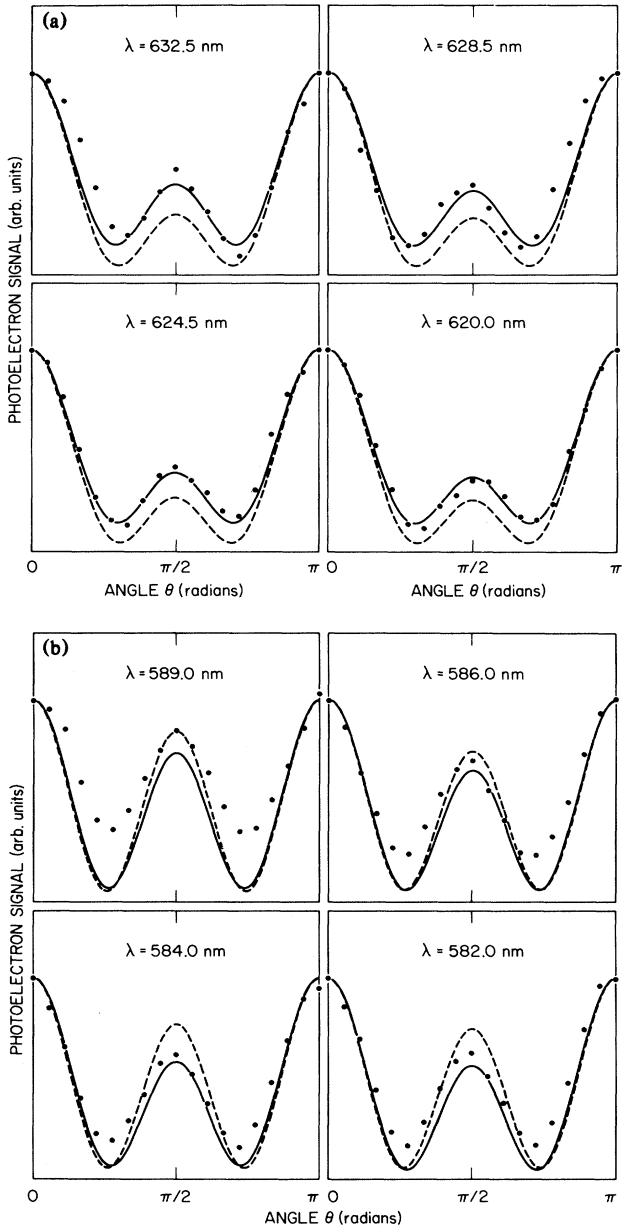

FIG. 2. Photoelectron angular distributions for nonresonant two-photon ionization of (a) cesium atoms and (b) rubidium atoms. The error bars are three times the size of the dot. The solid lines are the theoretical calculations using the Sturmian-basis-set method and the dashed curves are from the Hartree-Fock procedure.

determined by least-squares fitting the data with Eq. (1). For cesium, the Sturmian procedure gives results which are actually in quite good quantitative agreement with the experimental results. In comparing the photoelectron angular distributions for the two atoms, we note that both experiment and theory find that the

TABLE I. Experimental and theoretical values of the β coefficients.

Alkali metals	λ (nm)	Photoelectron energy (eV)	Experiment β_2	Experiment β_4	Sturmian method β_2	Sturmian method β_4	Hartree-Fock method β_2	Hartree-Fock method β_4
Cesium	632.5	0.027	−3.18	4.42	−3.58	4.82	−4.99	7.35
	628.5	0.052	−3.29	4.78	−3.61	5.02	−5.08	7.65
	624.5	0.077	−3.29	4.87	−3.64	5.21	−5.14	7.90
	620.0	0.106	−3.55	5.43	−3.66	5.38	−5.22	8.16
Rubidium	589.0	0.033	−2.48	2.69	−3.69	4.32	−3.93	4.11
	586.0	0.055	−3.03	3.49	−4.11	4.65	−3.99	4.33
	584.0	0.069	−3.29	3.88	−4.15	4.87	−3.98	4.28
	582.0	0.084	−3.31	3.95	−4.32	5.09	−4.01	4.34

ratio of the intensity at $\theta = 90°$ to that at $\theta = 0°$ is larger in rubidium than in cesium for approximately the same value of photoelectron energy above the two-photon ionization threshold. We also note that in both atoms, this ratio decreases as the laser wavelength is decreased. The deviation of the data from the theory for photon energies nearest the threshold may be due to the difficulties with detection of ultraslow electrons or possibly due to neglect of electron correlation and relativistic effects in the calculations.

For the three-photon ionization of cesium, involving above-threshold ionization, a third photon is absorbed in the continuum. The differential cross section, $\sigma(\theta)^{(3)}$, is given by[19]

$$\sigma(\theta)^{(3)} = C^{(3)}(\cos^2\theta + \beta_4^{(3)}\cos^4\theta + \beta_6^{(3)}\cos^6\theta), \tag{3}$$

where $C^{(3)}$ is a normalization constant. The coefficients, $\beta_l^{(3)}$, are ratios of linear combinations of third-order matrix elements, $r_l^{(3)}$, and cosine functions of the difference in phase shifts between $l = 1$ and $l = 3$ continuum waves. For comparison with experiment we will again use the results of calculations which employed the Sturmian basis set[21] and Hartree-Fock procedures[24] in calculating the summation over intermediate virtual states.

The experimental and theoretical angular distributions obtained at a laser wavelength of $\lambda = 633.66$ nm are shown in Fig. 3. Both theoretical methods gave essentially identical results. The intensities are normalized at $\theta = 0°$. At $\theta = 0°$ the photoelectron peak corresponding to the three-photon above-threshold ionization was $\sim 1\%$ of that for the two-photon process. Four- and five-photon peaks were not detected. If present, their intensity is less than one-tenth that of the three-photon peak.

The measured angular distribution for the above-threshold ionization does not compare well with the theoretical calculations. The major discrepancy appears at $\theta = \pi/2$ where theory predicts zero intensity for any nonresonant multiphoton process involving an odd number of photons. It is important to note that Leuchs and Smith[7] have also observed a nonzero intensity at $\theta = \pi/2$ for five-photon nonresonant ionization of sodium. In our case, the nearest resonant intermediate state ($5d\,^2D$) is over 1000 cm^{-1} away from the first photon so that detuning far exceeds the spin-orbit coupling and the laser power is far too weak to allow for level shifting in and out of resonance. In addition, the polarization, P, of the laser was measured to be 0.99 at the laser focus. It is possible that space-charge and/or nonzero background effects coupled

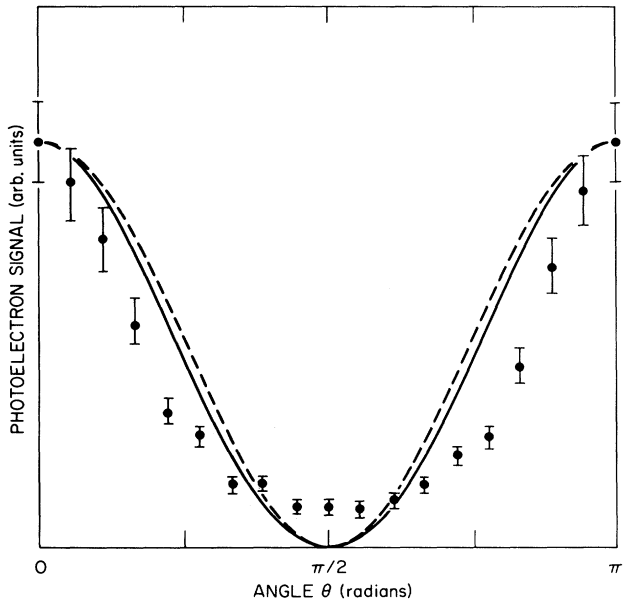

FIG. 3. Photoelectron angular distribution for above-threshold ionization in cesium at a laser excitation wavelength of 633.66 nm. The dots are the experimental values. The solid line is the theoretical calculation using the Sturmian-basis-set method and the dashed curve is from the Hartree-Fock procedure.

with the low signal level could partly account for the nonzero intensity at $\theta = \pi/2$. We note that the theory predicts primarily a $\cos^2\theta$ distribution whereas the experimental distribution contains contributions from higher-order terms. Further experimental and theoretical studies are in progress.

We wish to thank P. Lambropoulos and X. Tang of the University of Southern California and the University of Crete, and M. S. Pindzola of Auburn University for numerous helpful discussions and permission to include the theoretical calculations. This research was sponsored jointly by the Office of Health and Environmental Research, U. S. Department of Energy, under Contract No. DE-AC05-84OR21400, with Martin Marietta Energy Systems Inc., and the office of Naval Research, under Interagency Agreement No. N00014-85-F-0011.

[1]P. Lambropoulos, in *Advances in Atomic and Molecular Physics,* edited by D. R. Bates (Academic, New York, 1976), Vol. 12, pp. 87–164.

[2]*Multiphoton Processes,* edited by J. H. Eberly and P. Lambropoulos (Wiley, New York, 1978).

[3]*Multiphoton Ionization of Atoms,* edited by S. L. Chin and P. Lambropoulos (Academic, New York, 1984).

[4]J. A. Duncanson, Jr., M. P. Strand, A. Lindgrard, and R. S. Berry, Phys. Rev. Lett. **37**, 987 (1976).

[5]J. C. Hansen, J. A. Duncanson, Jr., R. L. Chien, and R. S. Berry, Phys. Rev. A **21**, 222 (1980).

[6]H. Kaminski, J. Kessler, and K. J. Kollath, Phys. Rev. Lett. **45**, 1161 (1980).

[7]G. Leuchs and S. J. Smith, J. Phys. B **15**, 1051 (1982).

[8]D. Feldmann and K. Welge, J. Phys. B **15**, 1651 (1982).

[9]R. Hippler, H.-J. Humpert, H. Schwier, S. Jetzke, and H. O. Lutz, J. Phys. B **16**, L713 (1983).

[10]R. N. Compton, J. A. D. Stockdale, C. D. Cooper, X. Tang, and P. Lambropoulos, Phys. Rev. A **30**, 1766 (1984).

[11]S. T. Manson and A. F. Starace, Rev. Mod. Phys. **54**, 389 (1982).

[12]J. Morellec, D. Normand, and G. Petite, in *Advances in Atomic and Molecular Physics,* edited by D. R. Bates (Academic, New York, 1982), Vol. 18, pp. 97–164.

[13]G. Petite, F. Fabre, P. Agostini, M. Crance, and M. Aymar, Phys. Rev. A **29**, 2677 (1984).

[14]P. Agostini, F. Fabre, G. Mainfray, G. Petite, and N. K. Rahman, Phys. Rev. Lett. **42**, 1127 (1979).

[15]P. Kruit, J. Kimman, and M. J. van der Wiel, J. Phys. B **14**, L597 (1981).

[16]F. Fabre, P. Agostini, G. Petite, and M. Clement, J. Phys. B **14**, L677 (1981).

[17]P. Kruit, H. G. Muller, J. Kimman, and M. J. van der Wiel, J. Phys. B **16**, 2359 (1983).

[18]P. Kruit, J. Kimman, H. G. Muller, and M. J. van der Wiel, Phys. Rev. A **28**, 248 (1983).

[19]P. Lambropoulos, Phys. Rev. Lett. **28**, 585 (1972).

[20]J. Mizuno, J. Phys. B **6**, 314 (1973).

[21]X. Tang and P. Lambropoulos, to be published.

[22]S. Klarsfeld and A. Maquet, J. Phys. B **12**, L553 (1979).

[23]E. Karule, J. Phys. B **11**, 441 (1978).

[24]M. S. Pindzola, private communication.

[25]M. S. Pindzola, Phys. Rev. A **17**, 1021 (1978).

[26]M. Aymar and M. Crance, J. Phys. B **14**, 3583 (1981).